Supplementary Materials:

	G90D-GαCT	G90D	G90D opsin
Data collection	SLS, x06sa	SLS, x06da	SLS, x06sa
Space group	H32	H32	H32
a, *b*, *c* (Å)	242.4, 242.4, 110.4	242.8, 242.8, 110.8	244.6, 244.6, 109.5
α, *β*, *γ* (°)	90, 90, 120	90, 90, 120	90, 90, 120
Resolution (Å)	40-2.9 (3.07-2.9) [a]	40-3.3 (3.47-3.3) [a]	40-3.9 (4.08-3.9) [a]
R_{pim} (%)	7.4 (49.1)	7.9 (47.3)	10.5 (53.4)
$I/\sigma I$	9.9 (1.55)	9.0 (1.43)	6.5 (1.38)
CC(1/2) (%)	99.6 (61.2)	99.6 (61.8)	99.7 (67.3)
Completeness (%)	99.6 (98.4)	99.4 (97.4)	99.8 (99.5)
Multiplicity	27.9 (27.9)	20.2 (20.5)	9.6 (9.8)
Refinement			
No. reflections	27501 (4299)	18833 (2615)	11340 (1399)
R_{work}/ R_{free}	0.231/0.255	0.2292/0.2443	0.299/0.334
No. atoms	2817	2703	2592
B-factors (Å^2)			
Macromolecule	56.08	55.68	96.7
Solvent	46.63	50.26	
R.m.s deviations			
Bond lengths (Å)	0.012	0.011	0.011
Bond angles (°)	1.68	1.601	1.16
MolProbity score/percentile	2.21/98th	2.26/97th	3.01/88th

[a] highest resolution shell is shown in parenthesis

Table S1. Data collection and refinement statistics. Data were collected from single crystals following a low-dose/high redundancy data collection strategy. To adequately reflect data improvement through a high redundancy data collection strategy, I/σ_I, R_{pim} and the correlation factor CC(1/2) between random half-datasets were used to define resolution cutoffs [1].

Comparison	Overall	TM2 + TM7-H8	Retinal contacts	GαCT contacts
G90D-GαCTα to G90D	0.348	0.308	0.169	0.492
G90D-GαCT to Meta-II-GαCT	0.261	0.210	0.262	0.227
G90D-GαCT to Opsin-GαCT	0.667	0.543	0.322	0.309
G90D to Opsin	0.515	0.546	0.266	0.664

Table S2. Root mean square deviations (rmsd) of Cα atoms between structures of the G90D mutant with metarhodopsin-II (4A4M [2]) and structures of the apoprotein opsin with (3DQB [3]) and without the GαCT peptide (3CAP [4]). In addition to the complete structure, rmsd values have been calculated for helices TM2/TM7/H8 (residues 71-101 and 284-326) that are directly impacted by the formed G90D-K296 salt-bridge, amino acids in contact with retinal or the GαCT peptide (defined as having a distance of < 4 Å in the 4A4M metarhodopsin-II structure).

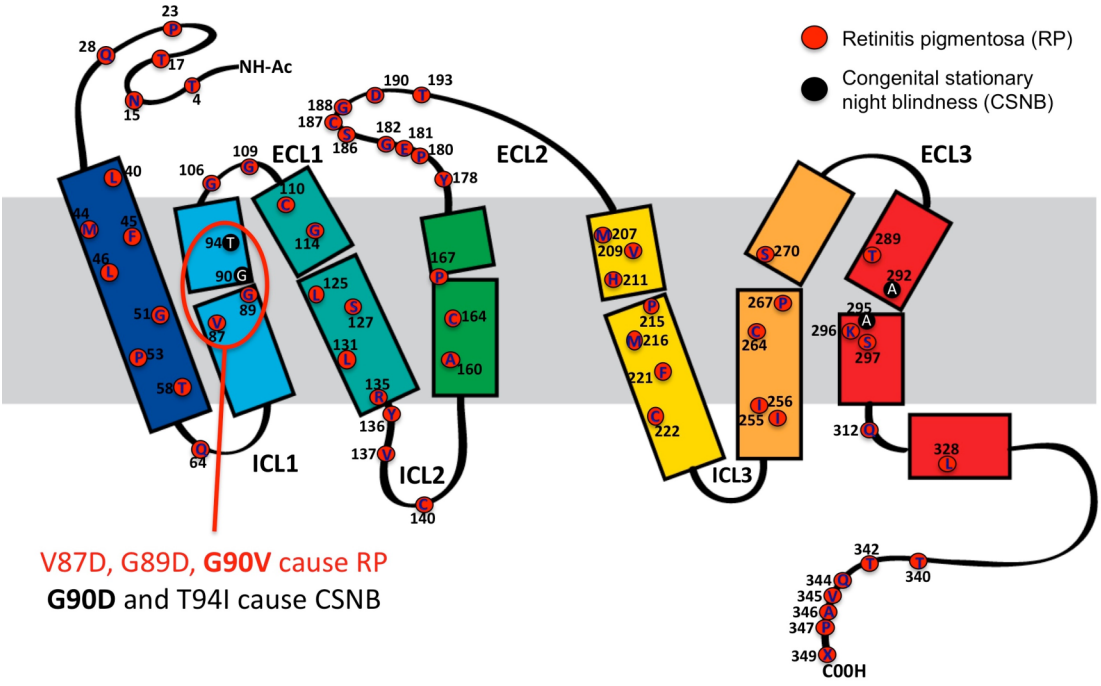

Fig. S1: Point mutations in rhodopsin that cause blindness. Mutations lead to either RP (red circles), characterized by initial night blindness and a slow progression towards loss of day light vision, or CSNB (black circles), a milder form of the disease that is limited to impairment of night vision. While RP mutants are distributed over most of the polypeptide chain, the four known CSNB mutants are found close to the helical kinks in TM2 and TM7 that form part of the retinal-binding pocket. Mutations at position 90 are unique as they can cause either RP or CSNB providing a natural locus at which to study the molecular causes of retinal degeneration.

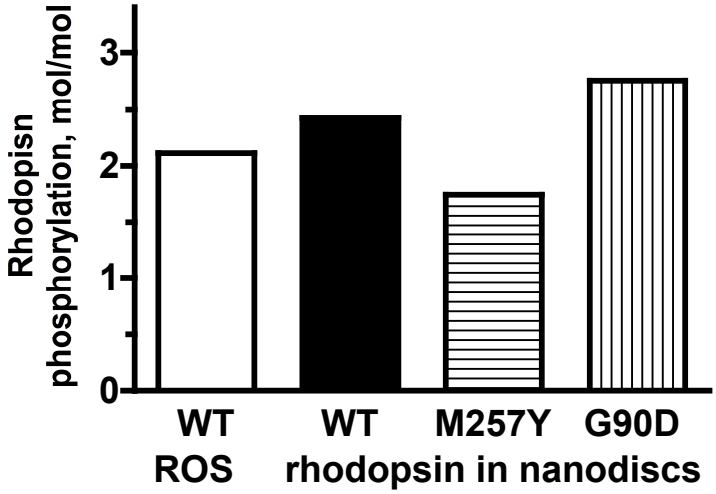

Fig. S2: Phosphorylation levels of light-activated rhodopsin in rod outer segment (ROS) membranes and of WT, M257Y and G90D in nanodiscs. Both wild type and the two constitutively active rhodopsin mutants reach similar phosphorylation levels as obtained with native rhodopsin in ROS membranes under identical conditions. However, the M257Y mutant that stabilizes the E(D)RY motif as part of the G_t binding site [2] reaches only 68% and 60% of the phosphorylation levels obtained with WT and the G90D mutant, respectively, suggesting that M257Y mutation may bias rhodopsin against GRK1. A representative experiment out of two performed in duplicates is shown.

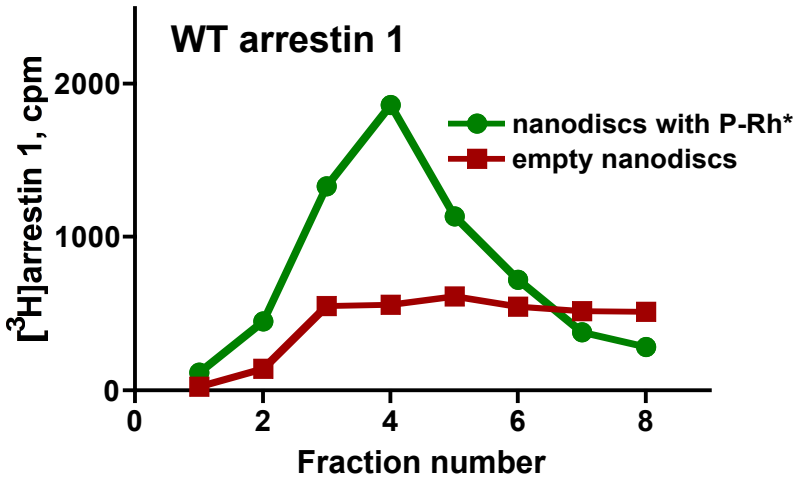

Fig. S3: Elution profile of arrestin-binding assays. Fraction 1 was 0.5 ml, all following fractions were 0.1 ml each. A representative experiment out of two performed in duplicates is shown.

Single event noise and the conformation of a G90D preactivated dark state

Based on dark current measurements in mice carrying a single copy of the G90D gene, the equivalent background light has been estimated to be 82-130 activated rhodopsins/rod/s [5,6]. Thus, basal activity of only a few of the 10^8 rhodopsin molecules present in a rod cell can produce a maintained activation of the signaling cascade leading to the night blindness observed in CSNB patients. With the active species present in minuscule amounts, it has been very difficult to locate the exact source of the stimulatory signal (see main discussion and Fig. 5). Much points towards a pre-activated rhodopsin dark state as source of the stimulatory signal. Including FTIR spectroscopy [7], spin label experiments [8] and increased hydroxyl amine reactivity indicating a perturbation of the G90D dark state [5]. Additionally, the pathologic phenotype in rods isolated from transgenic mice is not reversed after addition of 11-*cis*-retinal, even though regeneration was expected to deactivate constitutively active G90D opsin [6], as experiments with rods isolated from transgenic frogs suggested [9]. In contrast to previous experiments in COS cells [10] or experiments in transgenic frogs, the G90D mutation did not lead to higher constitutive activity in the transgenic mice. In agreement with these results, desensitization in G90D patients is not reversed even after 12 h of dark adaptation, a time span during which all G90D opsin should be regenerated and deactivated by 11-*cis*-retinal [11]. It is worth noting that the G90D dark state shows no increased G_t activation *in vitro* [10]. This may not be necessary, as a very low level of basal activity (~100 active molecules out of 10^8 rhodopsins in the rod) is sufficient to yield the CSNB phenotype [5,6]. Interestingly, no increase in single event noise was detected in mice expressing G90D rhodopsin [6] pointing towards a constant activation with low gain. In this respect it should be noted that electrophysiological detection is only suitable for events that mimic light activation of rhodopsin, such as thermal isomerization of retinal, which yield rhodopsin molecules with the lifetime of the active state sufficient to activate 40-50 G_t molecules, producing a "single photon response" of the amplitude that can be detected. Our data suggests that the G90D dark state is likely to be structurally very dynamic, so that its active-like state might exist a very short time sufficient to activate very few G_t molecules at a time, which would produce no electrophysiologically detectable noise. Importantly, for the rod 10 short-lived "active" mutants each activating 4-5 G_t would have the same desensitizing

effect as one active rhodopsin with normal lifetime. A very short lifetime of active-like state of the mutant would also render a normal desensitization mechanism inefficient: rhodopsin needs to remain active long enough for GRK1 to attach 3 or more phosphates necessary for high-affinity arrestin-1 binding [12,13]. Short-lived active-like rhodopsin is unlikely to be multi-phosphorylated, and therefore would escape the normal quenching mechanism. Collectively, the absence of electrophysiologically detectable noise along with measurable rod desensitization [5,6] strongly argue for a very short-lived active-like state of the mutant. This is consistent with the lower stability of the G90D dark state and its inability to crystallize, suggesting a highly dynamic molecule where both inactive and active dark states are unstable.

Materials and Methods:

Protein expression

For expression we stably transfected the cDNA of bovine rhodopsin into HEK293GnTI$^-$ cells [14] cells with restricted and homogenous N-glycosylation [14,15]. In addition to the G90D mutation, we introduced the N2C/D282C double substitution that increases thermal stability but does not change retinal binding, G_t activation [16], activation pathways [17] or structure [18]. This functionally neutral background is unique among GPCRs and offers the possibility to investigate the structural impact of disease causing mutations in a native as well as biochemically and spectroscopically well defined system with homogenous posttranslational modifications. We used 1D4-coupled resin to purify N2C/G90D/D282C rhodopsin either as the apoprotein opsin or in the 11-*cis*-retinal reconstituted dark state.

Cells were expanded as adhesion cultures in DMEM/F12 medium (Invitrogen) supplemented with FBS (10%), PenStrep (Gibco), Geneticin-G418 (200µg/ml) and blasticidin (5µg/ml). Cells were harvested and further expanded as suspension cultures in a 10l wave bioreactor (GE Healthcare) containing PEM medium (Invitrogen) supplemented with FBS (10%) and PenStrep (Gibco). When a cell density of $2x10^6$ cells/ml was reached, protein expression was induced by addition of 2µg/ml tetracycline and 5mM sodium butyrate. Cells were harvested after 72 h and stored at -80°C.

Receptor purification

Cell pellets were solubilized for 1 hour at 4°C with PBS buffer containing protease inhibitors (complete protease inhibitor cocktail tablets, Roche) and 1.25% DM (β-decyl-maltoside). Opsin was bound to 1D4 antibody [15,19] coupled to CNBr-activated Sepharose 4B resin (GE Healthcare) and washed with PBS pH 7.0, 0.125% DM. The resin was incubated overnight at 4°C with 11-*cis* retinal (50 μM) to reconstitute dark state rhodopsin. All steps involving retinal were performed under dim red light. The resin was washed with PBS pH 7.0, 0.125% DM followed by 10mM HEPES pH 7.0, 0.125% DM. The purified protein was eluted in the same buffer supplemented with an elution peptide resembling the C-terminus of rhodopsin (TETSQVAPA, 80μM). For crystallization the buffer was exchanged on a Sephadex200 gel filtration column to 10mM sodium acetate pH 5.0, 100mM NaCl, 1% OG (β-octyl-glycoside). The apoprotein opsin was purified the same way as dark state rhodopsin, only without overnight incubation with 11-*cis*-retinal.

Light activation and crystallization

Reconstituted dark state rhodopsin was concentrated to 5-7.5 mg/ml (Vivaspin, 50kD cutoff concentrator). The sample was mixed with dried brain lipid extract (lipid to protein ratio of 0.5-1 w/w, Avanti Polar Lipids), briefly sonicated and incubated for 30 min in presence of a 10 fold molar excess of the GαCT2 peptide [1,19] resembling the last eleven amino-acids of the Gα subunit of the G_t carrying the K341L and C344V mutations (ILENLKDVGLF, Peptide 2.0 Inc). In addition to the 125-200 μM 11-*cis*-retinal prebound to the purified receptor, reactions contained 1μM all-*trans*-retinal. Just before crystallization, the receptor was selectively light activated for 5 minutes using a >475nm long pass filter that prevented exposure of free retinal and metarhodopsin-II. Free unprotonated 11-*cis*-retinal that has been released during purification of G90D does not absorb at this wavelength, which may explain the residual 11-*cis*-retinal contribution shown in the electron density obtained from the light-activated mutant. The light activated protein was crystallized in the dark by sitting drop vapor diffusion against 3.0-3.5 M ammonium sulphate, 100 mM sodium acetate pH 4.5. Crystals were harvested under dim red light and soaked in crystallization buffer containing 10% trehalose prior to freezing in liquid nitrogen.

Crystals of opsin were obtained with the same procedure, except that all-*trans*-retinal and the light-activation step were omitted.

Data collection and structure determination

Data was collected using beamlines PXI-X06SA and PXIII-X06DA at the Swiss Light Source (SLS) following a fine slicing, low-dose/high redundancy data collection strategy. As R_{merge} values do not adequately reflect the quality of high redundant datasets, I/sI, R_{pim} and CC(1/2) values were used to define resolution cutoffs [1,20]. Data were integrated and scaled using XDS [20,21]. Phases were obtained by molecular replacement using the program PHASER [2,21] and the polypeptide of the previously crystallized M257Y mutant [2,22] as search model. The resulting solution was refined using iterative cycles of model building in COOT [22,23] and refinement (rigid body, energy minimization, simulated annealing, individual B-factor refinement) with the PHENIX program suite [23,24]. Coordinates and structure factors have been deposited under pdb code 4bey for G90D-GαCT2, 4bez for G90D.

Thermal shift assay

Thermal shift assays were performed in an Eclipse fluorimeter (Varian) equipped with multisample holder. Thermal denaturation was followed using the thiol specific malemaide fluorochrome CPM (N-[4-(7-diethylamino-4-methyl-3-coumarinyl)phenyl]malemeide) as described [24]. Conditions were as follows, 2.5 µg of opsin purified by 1D4 immunoaffinity purification was diluted into 118 µl ice cold buffer (100 mM NaCl, 10 mM HEPES pH 7.5 and 0.125% DM) supplemented with either 10 µM 11-*cis*- or all-*trans*-retinal and incubated in the dark for 2 hours. Immediately before the measurement CPM (3mg/ml in DMSO) was diluted 1:30 into buffer and 10 µl of this mixture added to the reaction mix. Cuvettes were placed into the fluorimeter and fluorecence (Ex: 418nm, Em: 464 nm) measured while ramping temperature from 20° to 90°C at 2°C/min. The excitation wavelength was chosen to minimize interference with free retinal (380 nm) or protonated retinal in dark state rhodopsin (500 nm) while maintaining a strong CPM fluorescence signal. No change in rhodopsin absorption was detected in control experiments without temperature ramping. Melting curves were fitted using a sigmoidal Boltzmann equation to obtain

TM_{50} values. Average TM_{50} values and standard deviations were obtained from four measurements.

In vitro phosphorylation assay

Recombinant GRK1 was expressed and purified as described [25]. Rhodopsin in POPC nanodiscs with the indicated fraction of POPS (50 μg/ml), was phosphorylated in 20 mM Tris-HCl, pH 7.4, 3 mM $MgCl_2$, 10 μg/ml BSA, 0.5 mM ATP by purified GRK1 (2.5 μM) for 30 min at room temperature. Analytical reactions were performed in 10 μl with [γ-^{32}P]ATP (final specific activity 1,100–1,500 cpm/pmol), stopped by the addition of an equal volume of SDS sample buffer (2x, Sigma), and resolved on 10% PAGE. Gels were stained with Coomassie Blue, dried, and exposed to X-ray film for 1–3 h. Rhodopsin band was then excised, and the radioactivity was quantified in a liquid scintillation counter. Preparative reactions were performed in a volume of 120 μl (a 10 μl aliquot was added to [γ-^{32}P]ATP, incubated in parallel, and used to determine phosphorylation stoichiometry). Phosphorhodopsin was regenerated by the addition of 1 μl of 35 μM 11-*cis*-retinal followed by incubation in the dark at room temperature for 120 min.

Arrestin-1 binding to rhodopsin in nanodiscs

All arrestins were labeled during cell-free translation by incorporation of [^{3}H]leucine and [^{14}C]leucine, as described [26], with the specific activity of the mix 1.5-3 Ci/mmol leucine, resulting in the specific activity 51-102 Ci/mmol (113-226 dpm/fmol) of bovine arrestin-1, which contains 34 leucines. The translation of every mutant used in this study produced a single labeled protein band with the expected mobility on SDS-PAGE. The relative stability of all mutants was evaluated as described [27,28] and exceeded 90% of wild type bovine arrestin-1. Translated protein was separated from unincorporated labeled leucine by gel-filtration on 2-ml Sephadex G-75 columns. Protein fractions were pooled and used in the binding assay. Radiolabeled arrestin (100 fmol) was incubated in 50 mM Tris-HCl, pH 7.5, 0.5 mM $MgCl_2$, 1.5 mM dithiothreitol, 100 mM potassium acetate, and 7.5 pmol (0.3μg) of different functional forms of rhodopsin in nanodiscs in a final volume of 50 μl for 5 min at 30°C in the dark (dark forms) or in room light (light-activated forms and light-insensitive opsin). The samples were immediately cooled on ice and rhodopsin-bound

and free arrestin-1 was separated on 2-ml Sephadex G-100 columns equilibrated with 10 mM Tris-HCl, pH 7.5, 100 mM NaCl (in dim red light for dark forms). Nonspecific binding was determined in the presence of equal amount of empty nanodiscs and subtracted (Fig. S3).

References:

1. Karplus PA, Diederichs K. Linking crystallographic model and data quality. Science. 2012 May 25;336(6084):1030–3.

2. Deupi X, Edwards P, Singhal A, Nickle B, Oprian D, Schertler G, et al. Stabilized G protein binding site in the structure of constitutively active metarhodopsin-II. Proc. Natl. Acad. Sci. U.S.A. 2012 Jan 3;109(1):119–24.

3. Scheerer P, Park JH, Hildebrand PW, Kim YJ, Krauss N, Choe H-W, et al. Crystal structure of opsin in its G-protein-interacting conformation. Nature. 2008 Sep 25;455(7212):497–502.

4. Park JH, Scheerer P, Hofmann KP, Choe H-W, Ernst OP. Crystal structure of the ligand-free G-protein-coupled receptor opsin. Nature. 2008 Jul 10;454(7201):183–7.

5. Sieving PA, Fowler ML, Bush RA, Machida S, Calvert PD, Green DG, et al. Constitutive 'light' adaptation in rods from G90D rhodopsin: a mechanism for human congenital nightblindness without rod cell loss. J Neurosci. 2001 Jul 31;21(15):5449–60.

6. Dizhoor AM, Woodruff ML, Olshevskaya EV, Cilluffo MC, Cornwall MC, Sieving PA, et al. Night blindness and the mechanism of constitutive signaling of mutant G90D rhodopsin. J Neurosci. 2008 Nov 5;28(45):11662–72.

7. Zvyaga TA, Fahmy K, Siebert F, Sakmar TP. Characterization of the mutant visual pigment responsible for congenital night blindness: a biochemical and Fourier-transform infrared spectroscopy study. Biochemistry. 1996 Jun 11;35(23):7536–45.

8. Kim J-M, Altenbach C, Kono M, Oprian DD, Hubbell WL, Khorana HG. Structural origins of constitutive activation in rhodopsin: Role of the K296/E113 salt bridge. Proc. Natl. Acad. Sci. U.S.A. 2004 Aug 23;101(34):12508–13.

9. Jin S, Cornwall MC, Oprian DD. Opsin activation as a cause of congenital night blindness. Nat. Neurosci. 2003 Jul;6(7):731–5.

10. Rao VR, Cohen GB, Oprian DD. Rhodopsin mutation G90D and a molecular mechanism for congenital night blindness. nature. 1994 Feb 17;367(6464):639–42.

11. Sieving PA, Richards JE, Naarendorp F, Bingham EL, Scott K, Alpern M. Dark-light: model for nightblindness from the human rhodopsin Gly-90-->Asp mutation. Proc. Natl. Acad. Sci. U.S.A. 1995 Jan 30;92(3):880–4.

12. Mendez A, Burns ME, Roca A, Lem J, Wu LW, Simon MI, et al. Rapid and reproducible deactivation of rhodopsin requires multiple phosphorylation sites. Neuron. 2000 Oct;28(1):153–64.

13. Vishnivetskiy SA, Raman D, Wei J, Kennedy MJ, Hurley JB, Gurevich VV. Regulation of arrestin binding by rhodopsin phosphorylation level. J. Biol. Chem. 2007 Nov 2;282(44):32075–83.

14. Reeves PJ, Callewaert N, Contreras R, Khorana HG. Structure and function in rhodopsin: high-level expression of rhodopsin with restricted and homogeneous N-glycosylation by a tetracycline-inducible N-acetylglucosaminyltransferase I-negative HEK293S stable mammalian cell line. Proc. Natl. Acad. Sci. U.S.A. 2002 Oct 15;99(21):13419–24.

15. Molday RS, MacKenzie D. Monoclonal antibodies to rhodopsin: characterization, cross-reactivity, and application as structural probes. Biochemistry. 1983 Feb 1;22(3):653–60.

16. Xie G, Gross AK, Oprian DD. An opsin mutant with increased thermal stability. Biochemistry. 2003 Feb 25;42(7):1995–2001.

17. Standfuss J, Zaitseva E, Mahalingam M, Vogel R. Structural impact of the E113Q counterion mutation on the activation and deactivation pathways of the G protein-coupled receptor rhodopsin. J. Mol. Biol. 2008 Jun 27;380(1):145–57.

18. Standfuss J, Xie G, Edwards PC, Burghammer M, Oprian DD, Schertler GFX. Crystal structure of a thermally stable rhodopsin mutant. J. Mol. Biol. 2007 Oct 5;372(5):1179–88.

19. Choe H-W, Kim YJ, Park JH, Morizumi T, Pai EF, Krauss N, et al. Crystal structure of metarhodopsin II. Nature. 2011 Mar 31;471(7340):651–5.

20. Kabsch W. Xds. Acta Crystallogr D Biol Crystallogr. 2010 Jan 31;66(Pt 2):125–32.

21. McCoy AJ, Grosse-Kunstleve RW, Storoni LC, Read RJ. Likelihood-enhanced fast translation functions. Acta Crystallogr D Biol Crystallogr. 2005 Apr;61(Pt 4):458–64.

22. Emsley P, Cowtan K. Coot: model-building tools for molecular graphics. Acta Crystallogr D Biol Crystallogr. 2004 Nov 25;60(12):2126–32.

23. Adams PD, Grosse-Kunstleve RW, Hung LW, Ioerger TR, McCoy AJ, Moriarty NW, et al. PHENIX: building new software for automated crystallographic structure determination. Acta Crystallogr D Biol Crystallogr. 2002 Nov;58(Pt 11):1948–54.

24. Alexandrov AI, Mileni M, Chien EYT, Hanson MA, Stevens RC. Microscale fluorescent thermal stability assay for membrane proteins. Structure. 2008 Mar;16(3):351–9.

25. Huang C-C, Yoshino-Koh K, Tesmer JJG. A surface of the kinase domain critical for the allosteric activation of G protein-coupled receptor kinases. J. Biol. Chem. 2009 Jun 19;284(25):17206–15.

26. Gurevich VV, Benovic JL. Visual arrestin interaction with rhodopsin. Sequential multisite binding ensures strict selectivity toward light-activated phosphorylated rhodopsin. J. Biol. Chem. 1993 Jun 5;268(16):11628–38.

27. Reeves PJ, Kim J-M, Khorana HG. Structure and function in rhodopsin: a tetracycline-inducible system in stable mammalian cell lines for high-level expression of opsin mutants. Proc. Natl. Acad. Sci. U.S.A. 2002 Oct 15;99(21):13413–8.

28. Gurevich VV. The selectivity of visual arrestin for light-activated phosphorhodopsin is controlled by multiple nonredundant mechanisms. J. Biol. Chem. 1998 Jun 19;273(25):15501–6.